Modelling soil detachment rates in rainfed agrosystems in the south-central Pyrenees

M. López-Vicente*, A. Navas, J. Machín

Department of Soil and Water, Estación Experimental de Aula Dei – CSIC, Avda. Montañana 1005, 50059 – Zaragoza, Spain

Abstract

Distributed erosion models are potential tools for identifying soil sediment sources and guiding efficient Soil and Water Conservation (SWC) planning. However, the uncertainty of model predictions has yet to be resolved. Splash erosion is one of the most important mechanisms in soil loss. In this study, monthly splash detachment rates were predicted using the Morgan, Morgan and Finney (MMF) empirical erosion model and the more complex Revised Morgan, Morgan and Finney (RMMF) erosion model. These two models were used to assess active and abandoned fields in the Spanish Pyrenees. Land uses were barley fields, pasture, recently and old abandoned fields. Input parameters assessed were rainfall characteristics, soil properties, land forms, and land cover. The splash detachment rates predicted by the MMF and the RMMF models were higher for barley fields than for pasture and abandoned fields. However, the more complex RMMF model predicted lower splash detachment rates, especially in pastures. In contrast, runoff detachment was highest in old abandoned fields although rates were much lower than those of splash detachment. Moreover, soil detachment by runoff was low or equal to zero from November to May for the different

* Corresponding author. Tel.: +34 976 716100; fax: +34 976 716145
E-mail address: mvicente@eead.csic.es (M. López-Vicente)

land uses since the soil remained unsaturated during this period as a consequence of low rainfall intensities and soil surface roughness. Monthly values for total detachment were highest in barley fields, reaching a maximum of 17.2 and 16.9 Mg ha^{-1} in September and October. The mean annual detachment rates for barley, pastures and recently and old abandoned fields were 81.1, 0.8, 61.8 and 22.3 Mg ha^{-1}, respectively. The splash and runoff detachment rates of the RMMF model appeared to be sensitive to land cover factors, rainfall intensity and soil micro-topography, thus it is a better model for assessing soil detachment for various land uses. The comparison of erosion rates between the ^{137}Cs and the MMF and RMMF models shows that the models predict lower erosion rates due to the low estimated rates of the runoff transport capacity. However, the estimated and measured rates are in close agreement and are under the limit of the tolerable soil loss for soils under Mediterranean conditions.

Keywords: Splash Detachment; Runoff Detachment; Rainfed crop; MMF model; RMMF model; Soil erosion; Spanish Pyrenees.

1. Introduction

The detachment of soil particles from the impact of raindrops is the first stage in the erosion process and is the primary cause of erosion on short, steep slopes (Wu et al., 1996). Understanding the factors involved in splash and runoff detachment is needed to gain a greater understanding of the onset of soil erosion.

Intense convective storms with high rainfall intensities (rainfall rates > 50 mm h^{-1}) are frequent during the summer in the south-central Pyrenees (Sánchez et al., 2003). In Spain, Ayala-Carcedo and Iglesias (2000) showed that an increase in the number of heavy storms changed the temporal pattern of sediment load in streams. Thus storms and rainfall promote

49 the detachment of soil particles and thus more information on this process, which affects soil
50 productivity and sustainability, is urgently required. Moreover, Nearing et al. (2004) predict
51 that global warming will lead to a higher frequency of extreme weather conditions.
52 Soil degradation, caused by intensive agriculture, deforestation and land abandonment have
53 led to increased runoff and soil erosion in the Central Pyrenees (Navas et al., 2007). Rainfed
54 crops, such as cereals, cover important areas in the drier parts of Mediterranean countries and
55 occupy mountainous areas. Aggressive rainfalls on these slopping landscapes contribute to
56 erosion of cultivated lands. Furthermore, agriculture in semiarid areas suffers from strong
57 annual variations in crop yields that directly depend on rainfall volume and distribution and
58 soil quality during the growing season.
59 In northeastern areas of Spain, agriculture has been intensively developed over the last
60 centuries through severe deforestation. Important socio-economic changes in the middle of
61 the 20th Century led to the rapid abandonment of land. Deforestation in exchange for long-
62 term cultivation has led to the deterioration of soil quality in many diverse environments
63 worldwide (Lu et al., 2002). In addition, the agrarian policy of the European Union has
64 encouraged the abandonment of marginal, unproductive and degraded lands. During the peak
65 period of land abandonment, rivers and other waterways had high amounts of sediment and
66 this coincided with higher flood discharges (Valero-Garcés et al., 1999). In this region, severe
67 soil losses have been reported in abandoned lands (Navas et al., 2005) and, as a consequence,
68 the upper soil horizons have been completely eroded. This has contributed to changes in the
69 surrounding environment and increased the vulnerability of agrosystems because of
70 progressive soil loss (Sanchez-Marañón et al., 2002).
71 In general, soil degradation in areas of changing land use is relatively well studied (Machín
72 and Navas, 1995). Studies have described the processes that occur in abandoned fields and
73 their effects on infiltration, runoff, and erosion (Lasanta et al., 1995, Navas et al., 1997).

However, no information is available on the monthly splash and runoff detachment of soil particles in agricultural fields in the Pyrenees. Conservation of soil and improved management practices can be achieved with a detailed study of the risk factors involved in water erosion.

In this study, two empirical models were used to estimate monthly detachment rates from fields with different land uses in order to identify the land use that is more prone to soil detachment. The Morgan, Morgan and Finney (MMF) empirical model estimates soil particle detachment caused by raindrop impact. The more complex Revised Morgan, Morgan and Finney (RMMF) model estimates soil particle detachment caused by both raindrop impact and runoff. These models were modified to account for soil infiltration properties and surface micro-topography. A comparison of each model might identify the most accurate approach for revealing land uses which are most susceptible to erosion. These results may contribute to the development of guidelines for soil conservation in these rapidly changing agro-systems.

2. Materials and methods

2.1 Study area

In this study, 41 fields under four different land uses were chosen as representatives of the rainfed agro-systems in the south-central Pyrenees, Spain. The fields were located between 690 and 830 m above sea level in the “Lagos de Estaña” area of Huesca (Fig. 1a). The area has a Mediterranean continental climate that includes two periods of intensive rainfall, one in spring (April and May) and a second in autumn (September and October). Mean annual rainfall is 595 mm (estimated from the period 1993-2006) with an interannual oscillation of 404 mm in 2004 and 876 mm in 1996. The mean annual temperature is 12.8 ºC with the coldest month being January (mean 4.2 ºC) and the hottest month being July (mean 21.6 ºC). López-Vicente et al. (2005) calculated monthly rainfall and temperature using data from the

Benabarre and Camporrélls weather stations for the period 1993-2004; weather data from 2005 and 2006 were also included in this study.

From the 41 fields, twelve were old abandoned fields (6.1 ha; more than 50 years ago), nine were more recently abandoned fields (5.7 ha; less than 20 years ago), 10 were cultivated with winter barley (12.8 ha), and ten were used for pasture (4.3 ha) (Fig. 1b). The old abandoned fields were covered with mature shrubs, especially *Buxus sempervirens*, and young evergreen oaks (*Quercus rotundifolia*), deciduous oaks (*Quercus faginea*) and kermes oaks (*Quercus coccifera*). Recently abandoned fields were sparsely covered with shrubs of *Buxus sempervirens*, *Juniperus oxicedrus* and sub-Mediterranean plants.

Soils were identified as Calcisols, Leptosols, haplic Regosols, gypsic Regosols, Gleysols and Gypsisols (Machín, personal communication, 2007). López-Vicente et al. (2005) measured the saturated hydraulic conductivity and matrix flux potential for each type of soil (Table 1).

2.2 The MMF and RMMF empirical erosion models

The MMF soil erosion model, which was proposed as a simple empirical model for predicting annual soil loss (Morgan et al., 1984), has the advantage of being easy to understand and data are readily available. The MMF model has been used in different areas of the world and has been the basis for other models such as the SEMMED model (Soil Erosion Model for Mediterranean Areas) proposed by De Jong et al. (1999) and used in southern France and Italy. The RMMF model of Morgan (2001) was validated using erosion plot data from 16 countries (Vigiak et al., 2006). Table 2 describes the input parameters of the MMF and RMMF models for assessing the splash and runoff detachment rates.

Estimation of rainfall energy and runoff

The energy of the rainfall in the MMF model (E; J m^{-2}) is based upon the kinetic energy (KE; J m^{-2} mm^{-1}) and the amount of the annual rainfall (R; mm) given by:

$$E = R\,KE \tag{1}$$

In the RMMF model the procedure for calculating rainfall energy was revised to take into account rainfall partitioning during interception and the energy of the leaf drainage. The effective rainfall (ER; mm) is computed from the annual total rainfall and the proportion (between 0 and 1) of the rainfall which reaches the ground after allowing for rainfall interception (A).

$$ER = R\,A \tag{2}$$

The effective rainfall ER is then separated into rainfall reaching the ground surface as direct throughfall (DT; mm) and as leaf drainage (LD; mm). This separation is a direct function of the percentage canopy cover (CC):

$$DT = ER - LD \tag{3}$$

$$LD = ER\,CC \tag{4}$$

The energy of the direct throughfall [$E(DT)$, J m-2] is determined as a function of rainfall intensity (I, mm h-1) using a typical value for the erosive rainfall of the region. Although the original version of the MMF model used the relationship of Wischmeier and Smith (1978), the enhanced version of the model proposes alternative equations based on local rainfall energy–intensity relationships. In this paper the equation developed by Coutinho and Tomás (1995) in southern Portugal has been selected for calculating the kinetic energy in the MMF and the RMMF models:

$$KE = 35.9\left[1 - 0.56\exp\left(-0.034I\right)\right] \tag{5}$$

$$E\left(DT\right) = DT\,KE \tag{6}$$

The energy of the leaf drainage [$E(LD)$; J m-2] is a function of the height of the plant canopy (PH; m) as proposed by Brandt (1990):

$$E(LD) = (15.8\, PH^{0.5}) - 5.87 \quad (7)$$

The total energy of the effective rainfall (EE; J m^{-2}) is obtained from:

$$EE = E(DT) + E(LD) \quad (8)$$

The procedure for estimating the runoff per raster cell (Q_i; mm) is the same for the two models based on the method proposed by Kirkby (1976) which assumes that runoff occurs when the daily rainfall exceeds the soil moisture storage capacity (R_C; mm). The monthly runoff Q_m is obtained from:

$$Q_m = R_m \exp(-R_C / R_0) \quad (9)$$

$$R_0 = R / R_n \quad (10)$$

where R_0 is the mean rainfall per erosive rain day (mm) and R_n is the annual number of days with erosive rainfall. Soil moisture storage capacity is estimated as:

$$R_C = 1000\, MS\, BD\, EHD\, (E_t / E_0)^{0.5} \quad (11)$$

where MS is soil moisture content at field capacity (% on weight basis), BD is the bulk density of the soil (Mg m^{-3}), EHD is the effective hydrological depth of the soil (m) and E_t / E_0 is the ratio between actual and potential evapotranspiration. EHD indicates the depth of the soil within which moisture storage capacity controls the generation of runoff and is a function of soil type and plant cover which influence the depth and density of roots.

The estimated runoff volume in Eq. (9) was modified by accounting for the amount of rainfall that is necessary to pond the soil (Rp_i, mm) and the maximum surface storage capacity (SS_{max}, mm). Hogarth et al. (1991) proposed that time to ponding (Tp, s) has a minimum and a maximum time and state that the average value can be calculated as:

$$\frac{1}{2}\frac{S_m^2}{K_{fs}} \ln\left(\frac{I_m}{I_m - K_{fs}}\right) \le Tp_m \le \frac{1}{2}\frac{S_m^2}{I_m - K_{fs}} \quad (12)$$

$$S_m = \sqrt{2(\Delta\theta_m)\phi} \quad (13)$$

$$\Delta\theta_m = \theta_S - \theta_{0m} \quad (14)$$

where S_m (mm $s^{-0.5}$) is the monthly soil sorptivity, K_{fs} (mm s^{-1}) is the saturated hydraulic conductivity, I_m (mm s^{-1}) is the monthly rainfall intensity, ϕ is the matrix flux potential (mm^2 s^{-1}) of each soil type and θ_S and θ_{0m} is the volumetric water content at saturation and initial conditions. The monthly rainfall volume to ponding (Rp_m, mm) was calculated by multiplying I_m by Tp:

$$Rp_m = Tp_m\, I_m \quad (15)$$

The maximum monthly surface storage capacity ($SS_{max\text{-}m}$, mm) was calculated according to Driessen (1986). This includes surface roughness (RG_m; mm), slope steepness (S; degree) and the surface furrow and ridge angle determined by tillage marks and micro-topography (SIG; degree). The effective volume of monthly runoff ($Q_{m\text{-}eff}$, mm) was calculated after the subtraction of Rp_m and $SS_{max\text{-}m}$ from the initial value of monthly runoff per raster cell (Q_m):

$$SS_{\max-m} = 0.5\, RG_m\, \frac{\sin^2(SIG - S)}{\sin(SIG)}\, \frac{\cot(SIG + S) + \cot(SIG - S)}{2\cos(SIG)\cos(S)} \quad (16)$$

$$Q_{m-eff} = \left(Q_m - Rp_m\, EE_m - SS_{\max-m}\, EE_m\right) \quad (17)$$

where EE_m is the number of erosive events per month m, and takes into account the effect of the monthly distribution of erosive events along the year. A SIG value of 30 º was considered valid for the study area based on Terzoudi et al. (2007). Surface roughness is the configuration of the soil caused by the randomly orientated arrangement of soil clods. Tillage tools can produce random roughness and orientated roughness. In this work the roughness values for forest areas (random roughness, RG = 20.3 mm) and cultivated fields with plough (RG = 48.3 mm) and field cultivator (RG = 17.8 mm) were taken from Renard et al. (1997).

Splash and runoff detachment rates

The splash detachment rate (F; kg m^{-2}) in the MMF model is calculated as:

$$F = K\left[E\exp(-aA)\right]^{b}10^{-3} \quad (18)$$

where K is the soil detachability index (g J^{-1}), a is a coefficient (a = 0.05) and b is an exponent (b = 1.0). The values of a and b in Eq. (18) correspond to those proposed by Quansah (1981) and used by De Jong et al. (1999). K depends on the particle size distribution of the soil and is adopted from the MMF model guide (Morgan, 2001; Table 3). In the RMMF model, soil particle detachment by raindrop impact (F; Kg m^{-2}) is defined as:

$$F = K\ EE\,10^{-3} \quad (19)$$

The RMMF model includes a component to assess the effect of runoff on soil detachment (H; kg m^{-2}) as a function of soil resistance (Z, kPa^{-1}), runoff (Q_i; mm) and slope steepness (S; radian). Soil detachment from runoff was estimated using the equation proposed by Quansah (1982) and modified by Morgan (2001):

$$H = Z\,Q_{m-eff}^{1.5}\sin(S)(1-GC)10^{-3} \quad (20)$$

$$Z = \frac{1}{0.5\,COH} \quad (21)$$

where GC is the amount of ground cover (%) and COH is the cohesion of the soil (kPa). The GC factor includes crop residue, rocks and other non-erodible material that is in direct contact with the soil surface. The COH is an important component of the soil's resistance to erosion based upon soil texture (Table 3).

Finally, the soil particle detachment rates by splash and runoff are summed to produce a total detachment rate. For the fields with the highest detachment rates, a method to validate the reliability of the predictions was made through an estimation of the transport capacity of the runoff (TC; kg m^{-2}) using the following equation:

$$TC = C\ \ P\,Q_{m-eff}^{d}\sin(S)10^{-3} \quad (22)$$

where C (–) and P (–) are the cover-management and the support practice factors, respectively, of the Revised Universal Soil Loss Equation (RUSLE) (Renard et al., 1997), and d is an exponent equal to 2 (Morgan, 2001).

Final soil loss predictions are computed on the basis of the conceptual model of Meyer and Wischmeier (1969) by comparing the rates of total detachment and runoff transport capacity. The lower of the two values per raster cell is assigned as the annual soil loss rate:

$$Mean\ Annual\ Soil\ Loss = \min\{(F + H), TC\} \quad (23)$$

2.3 Data collection

Monthly rainfall values were calculated using daily precipitation values from the Benabarre and Camporrélls weather stations. Intensity of erosive rain was obtained from rainfall data recorded every 15 min at the Canelles Weather Station for the period 1993 – 2006. These weather stations are 10.1, 7.5 and 11 km northwest, south and southeast from the study area, respectively. Erosive storms were distinguished from other events by comparing the amount and intensity of rainfall to thresholds proposed by Renard et al. (1997) in the RUSLE soil erosion guide. Data defined as erosive storms was used to calculate the typical value of the intensity of erosive events (I in Eq. 5) and the mean rainfall per erosive rainday (R_0 in Eq. 9 and 10).

A total of 54 soil samples were collected from the 41 fields. To determine the textural class of each sample, laser equipment was used and the corresponding values of K (Eqs 18 and 19) and COH (Eq. 21) were estimated based on the model guide (Morgan, 2001). The bulk density, BD (Eq. 11), and soil moisture content at field capacity, MS (Eq. 11), was measured for each sample using a porous ceramic plate in a closed chamber. The volumetric content of water at saturation was calculated for each soil sample and initial conditions were measured in June, August, December and February as representatives of seasonal variations.

242 The values of effective hydrological depth, *EHD* (Eq. 11), for each land use were calculated
243 using the data of López-Vicente et al. (2005) for each soil type (Table 4). These authors
244 calculated the ratio between actual and potential evapotranspiration (E_t / E_0 in Eq. 11) using
245 the Penman-Monteith and Priestley-Taylor equations for the different land uses (Table 4).
246 The slope steepness parameter (*S* in Eqs 16, 20 and 22) for each land use (Table 4) was
247 calculated using the slope map derived from an enhanced digital elevation model of the study
248 area (López-Vicente and Navas, 2005) at high spatial resolution (cell size: 5 x 5 m).
249 Rodríguez and Schnabel (1998) cited an average rainfall interception value of 22.5 % for a
250 Mediterranean forest of *Quercus ilex* in the Castanya experimental basin (Montseny, province
251 of Barcelona, NE Spain). Belmonte and Romero (1998) estimated the net rainfall interception
252 at 30.8 % in scrublands of southeastern Spain. These data were adopted for the old and more
253 recently abandoned fields, respectively (Table 4). Reliable data to parameterize pasture
254 species and crops were difficult to find. Eberbach and Pala (2005) obtained a rainfall
255 interception of 14 % for barley fields in northern Syria with a mean annual rainfall of 330 mm
256 during March, April, May and June. Alternatively, a rainfall interception of 3 % for crop
257 residues was estimated by Cook et al. (2006) during the months of July and August. It was
258 assumed that the months of September and October have a value of 0 due to plowing and
259 values for the months of November, December, January and February increase gradually from
260 0 to maximum 14 % until the month of March. Ashby (1999) measured a rainfall interception
261 of 8.33 % in pastures with a mean plant height (*PH* in Eq. 7) of 0.28 m (Table 4). The height
262 of the plant canopy for barley fields ranged from a minimum of 0 to a maximum of 0.46 m
263 with a mean value of 0.1 m (Renard et al., 1997) (Table 4). The *PH* parameter of the old and
264 recent abandoned fields (Table 4) was estimated using data from southern France (Rambal et
265 al., 2003).

Rodríguez-Calcerrada et al. (2007) measured the percentage of canopy cover at 80.7 % for the Mediterranean forest at Montejo de la Sierra in the Iberian Peninsula, whereas Carreiras et al. (2006) obtained a value of 27.5 % for the open Mediterranean forest and shrubs in a region of southern Portugal. These values were assigned to the old and recently abandoned fields, respectively. The canopy cover for barley fields was 30.42 % (Renard et al., 1997) whereas the value for pastures was 100 % due to the total soil coverage by this type of vegetation. The ground cover values for each land use were obtained from the percentage of coarse fragments calculated by López-Vicente et al. (2006) and percentage of soil surface covered by crop residues (Table 4).

The *C-RUSLE* factor, included in the crop cover parameter (*C* in Eq. 22), was calculated by López-Vicente et al. (2005) with the assistance of the *CropSyst 4.04.14* cropping simulator. Corresponding values were very low for the abandoned fields and moderate for cultivated fields (Table 4). The *P-RUSLE* factor, in absence of detailed data, was set to 1.

3. Results and discussion

3.1 Rainfall energy and runoff volume

A total of 74 storm events were recorded with 12 erosive storms (17 %) per year. The mean annual rainfall intensity calculated for the period 1993 – 2006 was 15.1 mm h^{-1}, with September having the highest average at 26.9 mm h^{-1} (Fig. 2a), and a maximum value of 69.8 mm h^{-1} for one single storm event. Usón and Ramos (2001) observed a mean rainfall intensity of less than 10 mm h^{-1} in northeastern Spain with a maximum of 103 mm h^{-1} for one single storm event.

The erosive storm events in September and October represented 53.5 % of the total (Fig. 2b). Rainfall intensity also varied seasonally. The most erosive storm events occurred from May to October with a mean intensity of 19.9 mm h^{-1}, whereas the mean value from November to

291 April was 7.4 mm h^{-1}. The mean annual rainfall per erosive rain day (R_0 in Eq. 9) was 47.2
292 mm.
293 After accounting for the effect of the rainfall interception and canopy cover parameters, the
294 volume of direct throughfall rainfall (*DT* in Eq. 3) was highest for barley fields, except in
295 May and June when the canopy cover parameter for this crop was very high. Moreover, the
296 volume of direct throughfall decreased with the age of abandonment of the fields. Old
297 abandoned fields had higher rainfall interception, canopy cover and plant height, without
298 seasonal variations. Pastures presented a minimum *DT* of zero, due to total soil coverage of
299 the canopy.
300 In the MMF model, a single monthly value of the rainfall energy for each land use was
301 calculated, whereas in the RMMF model, an individual temporal pattern for the total energy
302 of each land use was determined. The rainfall energy of leaf drainage represented 15.3, 1.7,
303 0.1 and 100 % of the total rainfall energy for old and recently abandoned fields, barley fields
304 and pastures, respectively. Barley fields exhibited the highest energy for direct throughfall
305 and total energy of the effective rainfall, and the lowest energy of leaf drainage. Total rainfall
306 energy decreased with increasing age of abandonment. Pastures gave the minimum value and
307 were more than 300 times lower than the annual value of barley fields. These results are
308 consistent with land uses that have greater canopy cover, percentage of interception, and
309 height of the plant canopy. The MMF model generated an annual value of kinetic energy that
310 was 1.5 times higher than the value generated by the RMMF model for barley fields.
311 The critical value of soil moisture storage (R_C in Eq. 11) was higher in the soils of barley
312 fields (34 mm) compared to old abandoned fields (24 mm). The effective hydrological depth
313 is the most important parameter to control soil moisture storage, however, variability was
314 very high in the soil samples collected in old abandoned fields. The results obtained by
315 Belmonte et al. (1999) in Murcia, Spain, in abandoned fields also agree with the results of the

316 present study. Old abandoned fields had the highest and barley fields the lowest monthly
317 runoff per raster cell (Q_m in Eq. 9). The temporal pattern of monthly runoff (Fig. 3a) was
318 correlated with monthly rainfall (Fig. 2a).
319 The estimated mean volumetric water content at saturation was 48.4 % and the mean
320 volumetric water content at initial conditions in June, August, December and February were
321 15.6, 10.6, 17.7, and 13.1 %, respectively. The values of time to ponding showed that soil did
322 not achieve saturation from December to March regardless of land use because the recorded
323 rainfall intensities were lower than the saturated hydraulic conductivity, in spite of similar
324 values of precipitation for the periods January to March and June to August (Fig. 2a).
325 Due to different K_{fs} values for the different land uses, runoff only took place from May to
326 October in the old abandoned fields, from July to September in the recently abandoned fields,
327 from April to November in barley fields, and from June to October in pastures. However, in
328 the months when rainfall intensity was higher than K_{fs}, the estimated time to ponding was
329 very short. Mean values were 4.5, 8.5, 8.2, and 13.1 s for old and recently abandoned fields,
330 barley fields and pastures, respectively. In the months when I_m is higher than K_{fs}, the
331 calculated rainfall volume to ponding, Rp_i, decreased by 0.1, 0.2, 0.1 and 0.4 % from the
332 initial runoff volume for the old and recently abandoned fields, barley fields and pastures,
333 respectively.
334 The maximum surface storage capacity, SS_{max}, varied with monthly rainfall and the amount of
335 water that remained on the soil surface was 12, 13, 22, and 12 % of the initial runoff volume
336 for old and recently abandoned fields, barley fields and pastures, respectively. The annual
337 volume of effective runoff was only 48, 21, 56, and 37 % of the initial annual runoff for old
338 and recently abandoned fields, barley fields and pastures, respectively. Hence, the combined
339 effect of infiltration properties and soil microtopography significantly reduced the amount of
340 runoff (Fig. 3b).

341

342 3.2 Soil detachment

343 The mean soil detachability index (*K* in Eqs 18 and 19) and cohesion (*COH* in Eq. 21) for
344 each land use are quite similar because all soils were silt loam (Fig. 4). Among the different
345 land uses, the MMF model predicted the highest monthly splash detachment rates for barley
346 fields with a total annual rate of 93.8 Mg ha^{-1} y^{-1} and a maximum of 18.1 and 17.8 Mg ha^{-1} in
347 September and October, respectively. The highest splash detachment rates for the period
348 February to June were associated with recently abandoned fields (Fig. 5a). The annual splash
349 detachment was quite similar for recently abandoned fields and pastures with 79.0 and 78.4
350 Mg ha^{-1} y^{-1}, respectively. The lowest rates were in February with 1.7 Mg ha^{-1} in the old
351 abandoned fields and 2.7 Mg ha^{-1} in the recently abandoned fields and pastures. Based on the
352 RMMF model, monthly splash detachment rates were highest in barley fields with maximum
353 rates of 17.2 and 16.8 Mg ha^{-1} in September and October, respectively (Fig. 5b). The annual
354 splash detachment rates for barley fields, old and recently abandoned fields and pastures were
355 80.8, 21.5, 61.6 and 0.3 Mg ha^{-1} y^{-1}, respectively. These values were lower than the annual
356 rate predicted with the MMF model, especially in pastures. In both models, splash detachment
357 rates were negatively correlated with abandonment. The highest splash detachment rates
358 occurred in September and October which were the months with the highest intensity and
359 volume of erosive rain and the lowest soil protection by canopy.
360 Barley and recently abandoned fields had the lowest monthly soil detachment by runoff (*H* in
361 Eq. 20) with annual rates of 0.23 and 0.28 Mg ha^{-1} y^{-1}, respectively. Higher annual
362 detachment rates occurred in pastures and old abandoned fields despite higher values of
363 ground cover with 0.84 and 0.56 Mg ha^{-1} y^{-1}, respectively (Fig. 5c). These results may be
364 explained by the higher soil cohesion and saturated hydraulic conductivity and the lower

slope steepness in barley fields. Therefore, slope steepness factor, rainfall intensity and infiltration properties are the most important parameters controlling runoff detachment rate.

As seen in Fig. 5d, values of total monthly detachment in old and recently abandoned fields and in barley fields are similar to splash detachment rates because of a low percentage of runoff detachment (3.8, 0.5 and 0.3 %, respectively). However, runoff detachment rates represented 68.7 % of total detachment rate in pasture despite this land use showing the lowest total detachment rate with an annual value of 0.8 Mg ha^{-1} y^{-1}. The maximum detachment rate occurred in barley fields. Maximum values were 17.2 and 16.9 Mg ha^{-1} in September and October and a total detachment rate was 81.1 Mg ha^{-1} y^{-1}. Annual detachment rates in old and recently abandoned fields were 22.3 and 61.8 Mg ha^{-1} y^{-1}, respectively.

Total detachment rates predicted with the RMMF model are lower than those predicted with the MMF model, especially in pastures. However, both models predicted the same temporal pattern of detachment for the different land uses (Fig. 5a and d). The RMMF model predicted maximum rates in September and October with 28, 29, 42, and 51 % of the annual rates in old and recently abandoned fields, barley fields and pasture, respectively. Both models also predicted lower detachment rates with increasing age of abandonment. Research by Navas et al. (2005) in old abandoned fields revealed that detachment rates were highest in soils on sunny orientated slopes with a low vegetative cover and high slope steepness. These results correspond with the predicted rates for the abandoned fields in the current study. Moreover, the decrease in detachment rates observed from recently to old abandoned fields in the south-central Pyrenees are similar to those observed in Almeria, Spain (Govers et al., 2006). In that study, land abandonment led to an exponential decrease in water erosion rates and sediment transport over 50-70 years. Navas et al. (1997) found higher soil displacement in cultivated and recently abandoned fields. Moreover, the negative effects of cultivation on erosion were

389 also observed in semiarid areas located in the same region of the study area (Quine et al.,
390 1994).
391 Temporal patterns observed in the current study were similar to that reported by Regüés and
392 Gallart (2004) at Vallcebre, southeast Pyrenees. In that study, sediment concentrations in
393 runoff samples were higher in spring and autumn than in winter and summer, and sediment
394 detachability by splash was higher in spring and autumn than in winter and summer.
395
396 3.3 Soil erosion and validation
397 To assess the reliability of the MMF and the RMMF model in estimating annual detachment
398 rates in barley fields, transport capacity by runoff was estimated (*TC* in Eq. 22) and the annual
399 soil loss rates were calculated (Eq. 23). These results were then compared with the erosion
400 rates measured by using fallout ^{137}Cs in eight soil samples that are included on an ongoing
401 research in the study area (Navas et al., personal communication, 2007). The mean values of
402 predicted and measured soil loss were 0.46 and 5.38 Mg ha^{-1} y^{-1}, respectively. Predicted soil
403 erosion rates were the same for both models and similar to values obtained by Morgan (2001)
404 in other Mediterranean agrosystems such as Italy (0.2 Mg ha^{-1} y^{-1}), Spain (0.49 Mg ha^{-1} y^{-1})
405 and Greece (< 0.01 Mg ha^{-1} y^{-1}). Morgan (2001) also found low rates for measured soil losses.
406 The low value of predicted soil erosion is explained by the low rate of runoff transport
407 capacity calculated with the RMMF model (Table 5). This is a limiting factor for estimating
408 annual erosion rate according to Eq. (23). Moreover, the estimated values of effective runoff
409 do not account for the erosive events from October to June when rainfall intensity is higher
410 than the saturated hydraulic conductivity because time to ponding was calculated with mean
411 values of I_m. Hence, the equations used to estimate the effective volume of runoff are
412 underestimating the actual volume of runoff and transport capacity, and thus, soil erosion
413 rates.

Tolerable soil loss (*T*) is defined as the maximum rate of annual soil erosion that will economically sustain a high level of crop productivity over the long-term. Boellstorff and Benito (2005) proposed a value of *T* between 1 and 13 Mg ha^{-1} y^{-1} for the majority of soils, whereas Renard et al. (1997) established a range between 2.2 and 11.2 Mg ha^{-1} y^{-1} for North American soils. In central Spain, De la Horra (1992) calculated a *T* value of 6 Mg ha^{-1} y^{-1} for the province of Toledo. The predicted soil erosion rate in barley fields with the RMMF model was lower than the *T* value proposed by De la Horra, whereas the measured rate with ^{137}Cs was almost equal to the maximum tolerable erosion rate.

4. Conclusion

Despite considerable variation in land cover factors, the temporal pattern of splash detachment rates with the MMF and the RMMF models are similar for the different land uses examined in this study. However, the predicted splash and total detachment rates were lower with the RMMF model than with the MMF approach, especially in pastures. The more complex approach of the RMMF model assessed the monthly detachment rate by raindrop impact using more accurate values, including temporal variability triggered by the different phases of tillage. Maximum surface storage capacity, time to soil ponding and rainfall to soil ponding play a key role in controlling runoff origin and volume and may explain the lack of runoff observed from December to March for the four types of land use.

The highest rates of runoff detachment occurred in old abandoned fields due to higher runoff volume, steeper slopes and lower soil resistance. Splash and total detachment rates were highest in barley fields and lowest in pastures although pastures and abandoned fields were located on steep hillsides. Moreover, old abandoned fields had lower splash and total detachment rates compared to recently abandoned fields. These results demonstrate that the more complex approach of the RMMF model provided a more accurate representation of the

erosive processes and is more sensitive to the detachment rates by raindrop impact and by runoff than did the simple approach of the MMF model. Hence, we conclude that land cover and intensity of erosive rainfall are more important in assessing splash and runoff detachment rates than mean monthly rainfall.

The average annual erosion rates obtained for barley fields with the two models were equal to and lower than the *T* value for soils under Mediterranean conditions due to an underestimation of the effective runoff volume. Further research is required to calculate the effective runoff volume at event scale for a more accurate assessment of runoff detachment and transport capacity. These results have implications for land conservation considering that current predictions of climate change will increase the frequency of extreme storm events, especially in Mediterranean areas. The high detachment rates that occurred in barley fields, with the maximum occurring between July and November, should be considered when designing and promoting better management practices aimed at preserving soil and water resources.

Acknowledgements

CICYT Projects REN2002-02702/GLO and CGL2005-02009/BTE funded this study.

References

Ashby, M., 1999. Modelling the water and energy balances of Amazonian rainforest and pasture using Anglo-Brazilian Amazonian climate observation study area. Agr. Forest Meteorol. 94, 79–101.

Ayala-Carcedo, F.J., Iglesias, A., 2000. Impactos del posible Cambio Climático sobre los recursos hídricos, el diseño y la planificación hidrológica en la España Peninsular (Impacts of possible climate change on water resources, design and hydrological planning

463 in Spain). In: Balairón (Ed.), El Cambio Climático. El Campo de las Ciencias y las Artes,
464 Servicio de Estudios del BBVA, Madrid, pp. 201–222.
465 Belmonte Serrato, F., Romero Díaz, A., 1998. La cubierta vegetal en las regiones áridas y
466 semiáridas: consecuencias de la interceptación de la lluvia en la protección del suelo y los
467 recursos hídricos (Canopy cover in arid and semiarid regions: consequences of rainfall
468 interception in soil protection and water resources). NORBA-Journal of Geography 10, 9–
469 22. Electronic journal (http://www.fyl-
470 unex.com/foro/publicaciones/norba/htm_esp/Index.html).
471 Belmonte Serrato, F., Delgado Iniesta, M.J., López Bermúdez, F., 1999. Interacciones entre el
472 suelo y la vegetación a lo largo de un transecto en un ecosistema semiárido (El Ardal,
473 Murcia) (Soil and vegetation interactions in a transect of a semiarid ecosystem (El Ardal,
474 Murcia)). Cuaternario y Geomorfología 13, 17–29.
475 Boellstorff, D., Benito, G., 2005. Impacts of set-aside policy on the risk of soil erosion in
476 central Spain. Agr. Ecosyst. Environ. 107, 231–243.
477 Brandt, C.J., 1990. Simulation of the size distribution and erosivity of raindrops and
478 throughfall drops. Earth Surf. Proc. Land. 15, 687–698.
479 Carreiras, J.M.B., Pereira, J.M.C., Pereira, J.S., 2006. Estimation of tree canopy cover in
480 evergreen oak woodlands using remote sensing. Forest Ecol. Manag. 223, 45–53.
481 Cook, H.F., Valdes, G.S.B., Lee, H.C., 2006. Mulch effects on rainfall interception, soil
482 physical characteristics and temperature under Zea mays L. Soil Till. Res. 91, 227–235.
483 Coutinho, M.A., Tomás, P.P., 1995. Characterization of raindrop size distributions at the Vale
484 Formoso Experimental Erosion Center. Catena 25, 187–197.
485 De Jong, S.M., Paracchini, M.L., Bertolo, F., Folving, S., Megier, J., de Roo, A.P.J., 1999.
486 Regional assessment of soil erosion using the distributed model SEMMED and remotely
487 sensed data. Catena 37, 291–308.

De la Horra, J.L., 1992. Aspectos biogeográficos en relación con la problemática agraria de la comarca de Torrijos (Toledo) (Biogeographic aspects in relation with the agricultural problematic in the region of Torrijos (Toledo)). Doctoral Dissertation. Universidad Complutense de Madrid, 653 pp.

Driessen, P.M., 1986. The water balance of soil. In: van Keulen, H., Wolf, J., (Eds.), Modeling of Agricultural Production: Weather, Soils and Crops. Pudoc, Wageningen, The Netherlands, pp. 76–116.

Eberbach, P., Pala, M., 2005. Crop row spacing and its influence on the partitioning of evapotranspiration by winter-grown wheat in Northern Syria. Plant Soil 268, 195–208.

Govers, G., Van Oost, K., Poesen, J., 2006. Responses of a semi-arid landscape to human disturbance: A simulation study of the interaction between rock fragment cover, soil erosion and land use change. Geoderma 133, 19–31.

Hogarth, W.L., Sardana, V., Watson, K.K., Sander, G.C., Parlange, J.Y., Haverkamp, R., 1991. Testing of approximate expression for soil water status at the surface during infiltration. Water Resour. Res. 27 (8), 1957–1961.

Kirkby, M.J., 1976. Hydrological slope models: the influence of climate. In: Derbyshire, E. (Ed.), Geomorphology and Climate. Wiley, London, pp. 247–267.

Lasanta, T., Pérez-Rontomé, C., García-Ruiz, J.M., Machín, J., Navas, A., 1995. Hydrological problems resulting from farmland abandonment in semiarid environments: the central Ebro depression. Phys. Chem. Earth 20, 309–314.

López-Vicente, M., Navas, A., 2005. Solving topography of Digital Elevation Model in karstic environments: a case study in the External Ranges of the Pyrenees. In: Gutiérrez, F., Gutiérrez, M., Desir, G., Guerrero, J., Lucha, P., Marín, C., García-Ruiz, J.M. (Eds.), Geomorphology in regions of environmental contrasts. Abstracts Volume of the Sixth International Conference on Geomorphology, Zaragoza, pp. 388.

López-Vicente, M., Nelson, R., Stockle, C.O., Navas, A., Machín, J., 2005. Modelización de la capacidad de transporte distribuida en subcuencas endorreicas del Pirineo oscense (Modelling distributed transport capacity in endorheic subcatchments of the Spanish Pyrenees). Proceedings of the II Simposio Nacional Sobre Control de la Degradación de Suelos. Madrid, Spain, pp. 813–817.

López-Vicente, M., Navas, A., Machín, J., 2006. Variation of soil erodibility in abandoned fields: A case study in the Carrodilla range (Spanish Pyrenees). In: Martínez-Casasnovas, J.A., Pla Sentís, I., Ramos Martín, M.C., Balasch Solanes, J.C. (Eds.), Soil and Water Conservation Under Changing Land Use, pp. 167–170.

Lu, D., Moran, E., Mausel, P., 2002. Linking Amazonian secondary succession forest growth to soil properties. Land Degrad. Dev. 13, 331–343.

Machín, J., Navas., A., 1995. Land evaluation and conservation of semiarid agrosystems in Zaragoza (NE Spain) using an Expert Evaluation System and GIS. Land Degrad. Rehabil. 6, 203–214.

Meyer, L.D., Wischmeier, W.H., 1969. Mathematical simulations of the process of soil erosion by water. T. ASAE 18, 905–911.

Morgan, R.P.C., 2001. A simple approach to soil loss prediction: a revised Morgan-Morgan-Finney model. Catena 44, 305–322.

Morgan, R.P.C., Morgan, D.D.V., Finney, H.J., 1984. A predictive model for the assessment of soil erosion risk. J. Agr. Eng. Res. 30, 245–253.

Navas, A., Garcia-Ruiz, J.M., Machin, J., Lasanta, T., Valero, B., Walling, D.E., Quine, T.A., 1997. Soil erosion on dry farming land in two changing environments of the central Ebro Valley, Spain. IAHS Publication, 245, 13–20.

536 Navas, A., Machín, J., Beguería, S., López-Vicente, M., Gaspar. L., 2007. Soil properties and
537 physiographic factors controlling the natural re-growth in a disturbed catchment of the
538 Central Spanish Pyrenees. Agroforest. Syst., DOI 10.1007/s10457-007-9085-2.
539 Navas, A., Machín, J., Soto, J., 2005. Assessing soil erosion in a Pyrenean mountain
540 catchment using GIS and fallout ^{137}Cs. Agr. Ecosyst. Environ. 105, 493–506.
541 Nearing, M.A., Pruski, F.F., O'Neal, M.R., 2004. Expected climate change impacts on soil
542 erosion rates: a review. J. Soil Water Conserv. 59, 43–50.
543 Quansah, C., 1981. The effect of soil type, slope, rain intensity and their interactions on
544 splash detachment and transport. J. Soil Sci. 32, 215–224.
545 Quansah, C., 1982. Laboratory experimentation for the statistical derivation of equations for
546 soil erosion modelling and soil conservation design. PhD Thesis, Cranfield Institute of
547 Technology.
548 Quine, T., Navas, A. Walling, D.E., Machín, J., 1994. Soil erosion and redistribution on
549 cultivated and uncultivated land near Las Bardenas in the Central Ebro River Basin,
550 Spain. Land Degrad. Rehabil. 5, 41–55.
551 Rambal, S., Ourcival, J.M., Offre, R.J., Mouillot, F., Nouvellon, Y., Reichstein, M.,
552 Rocheteau, A., 2003. Drought controls over conductance and assimilation of a
553 Mediterranean evergreen ecosystem: scaling from leaf to canopy. Global Change Biol. 9,
554 1813–1824.
555 Regüés, D., Gallart, F., 2004. Seasonal patterns of runoff and erosion responses to simulated
556 rainfall in a badland area in Mediterranean mountain conditions (Vallcebre, Southeastern
557 Pyrenees). Earth Surf. Proc. Land. 29, 755–767.
558 Renard, K.G., Foster, G.R., Weesies, G.A., McCool, D.K., Yoder, D.C., 1997. Predicting Soil
559 Erosion by Water: A Guide to Conservation Planning with the Revised Universal Soil

Loss Equation (RUSLE). Handbook #703. US Department of Agriculture, Washington, DC.

Rodríguez, A.B.M., Schnabel, S., 1998. Medición de la interceptación de las precipitaciones por la encina (*Quercus rotundifolia lam.*): metodología e instrumentalización. (Measurement of rainfall interception by oak trees (Quercus rotundifolia lam.): methodology and instrumentation). NORBA-Journal of Geography 10, 95-112. Electronic journal (http://www.fyl-unex.com/foro/publicaciones/norba/htm_esp/Index.html).

Rodríguez-Calcerrada, J., Pardos, J.A., Gil, L., Aranda, I., 2007. Summer field performance of Quercus petraea (Matt.) Liebl and Quercus pyrenaica Willd seedlings, planted in three sites with contrasting canopy cover. New Forest. 33, 67–80.

Sánchez, J.L., Fernádez, M.V., Fernández, J.T., Tuduri, E., Ramis, C., 2003. Analysis of mesoscale convective systems with hail precipitation. Atmos. Res. 67–68, 573–588.

Sanchez-Marañón, M., Soriano, M., Delgado, G., Delgado, R., 2002. Soil quality in Mediterranean mountain environments: effects of land use change. Soil Sci. Soc. Am. J. 66, 948–958.

Terzoudi, C.B., Gemtos, T.A., Danalatos, N.G., Argyrokastritis, I, 2007. Applicability of an empirical runoff estimation method in central Greece. Soil Till. Res. 92, 198–212.

Usón, A., Ramos, M.C., 2001. An improved rainfall erosivity index obtained from experimental interrill soil losses in soils with a Mediterranean climate. Catena 43, 293–305.

Valero-Garcés, B.L., Navas, A., Machín, J., Walling, D. 1999. Sediment sources and siltation in mountain reservoirs: a case study from the Central Spanish Pyrenees. Geomorphology 28, 23–41.

Vigiak, O., Sterk, G., Romanowicz, R.J., Beven, K.J., 2006. A semi-empirical model to assess uncertainty of spatial patters of erosion. Catena 66, 198–210.

585 Wischmeier, W.H., Smith, D.D., 1978. Predicting rainfall erosion losses, USDA Agricultural
586 Research Service Handbook 537.
587 Wu, T.H., Stadler, A.T., Low, C.W., 1996. Erosion and stability of a mine soil. J. Geotech.
588 Eng.-ASCE 122, 445–453.

589

590

591

592

593

594

595 Table 1. Saturated hydraulic conductivity (K_{fs}) and matrix flux potential (ϕ) for each soil type.

Soil type	K_{fs}	ϕ
	cm s^{-1}	cm^2 s^{-1}
Calcisol	0.0010	0.0182
Gleysol	0.0007	0.0009
Gypsic Regosol	0.0003	0.0006
Gypsisol	4.6E-5	0.0002
Haplic Regosol	0.0003	0.0033
Leptosol	0.0016	0.0011

596

597

598 Table 2. Input parameters for assessing soil detachment and transport capacity rates in the south-central Pyrenees
599 for the MMF and the RMMF erosion models.

Factor	Parameter	Model	Definition
Rainfall	R	MMF & RMMF	Rainfall (mm)
	I	MMF & RMMF	Typical value for intensity of erosive rain (mm h^{-1})
	R_0	MMF & RMMF	Mean rain per erosive rain day (mm)
Soil	K	MMF & RMMF	Soil detachability index (g J^{-1})
	COH	RMMF	Cohesion of the surface soil (kPa)
	MS	MMF & RMMF	Soil moisture content at field capacity (% w w^{-1})
	BD	MMF & RMMF	Bulk density of the top layer soil (Mg m^{-3})
	EHD	MMF & RMMF	Effective hydrological depth of the soil (m)
Landform	S	MMF & RMMF	Slope steepness (radian)
Land cover	A	MMF & RMMF	Rainfall intercepted by the vegetation and crop residue (%)
	E_t/E_0	MMF & RMMF	Ratio of actual (E_t) to potential (E_0) evapotranspiration
	CC	RMMF	Percentage canopy cover (%)
	GC	RMMF	Percentage ground cover (%)
	PH	RMMF	Plant height (m)
	C	MMF & RMMF	Cover – management factor in the RUSLE model (–)
Land use	P	MMF & RMMF	Support practice factor in the RUSLE model (–)

600

601 Table 3. Guide values of the soil parameters.

Soil texture	K	COH
	g J^{-1}	kPa
Sand	1.2	2
Loamy sand	0.3	2
Sandy loam	0.7	2
Loam	0.8	3
Silt	1.0	-
Silt loam	0.9	3
Sandy clay loam	0.1	3
Clay loam	0.7	10
Silty clay loam	0.8	9
Sandy clay	0.3	-
Silty clay	0.5	10
Clay	0.05	12

602

603 Table 4. Values of soil, landform and land cover parameters for the various land uses (see Table 2).

Land use	MS	BD	EHD	K	COH	E_t/E_0	A	CC	PH	GC	C	S
	% w w^{-1}	Mg m^{-3}	m	g J^{-1}	kPa	ratio	%	%	m	%	–	%
Old aband. field	0.352	1.34	0.087	0.874	3.31	0.32	22.5	80.7	5.5	0.36	0.004	21.8
Recently aband. field	0.309	1.23	0.119	0.873	3.44	0.33	30.8	27.5	1.0	0.36	0.022	19.9
Barley field	0.318	1.27	0.156	0.881	3.51	0.28	0 – 14	5 – 100	0 – 0.5	0.27	0.188	6.9
Pasture	0.332	1.18	0.138	0.869	3.58	0.33	8.3	100	0.3	0.30	0.123	24.5

604

605 Table 5 Mean monthly runoff transport capacity (*TC*; Mg ha^{-1} $month^{-1}$) for the various land uses estimated with
606 the MMF and RMMF models.

Land use	Jr	Fb	Mr	Ap	My	Jn	Jl	Ag	Sp	Oc	Nv	Dc	Annual
Old aband. field	0	0	0	0	0.012	0.003	0.002	0.005	0.014	0.016	0	0	0.052
Recently aband. field	0	0	0	0	0	0	0.010	0.019	0.053	0	0	0	0.081
Barley field	0	0	0	0.073	0.079	0.018	0.018	0.034	0.090	0.100	0.050	0	0.462
Pasture	0	0	0	0	0	0.011	0.011	0.021	0.059	0.067	0	0	0.169

607

608 Fig. 1. Location of the study area in the Huesca province, Spain (a), and location of the fields on the orthophoto
609 of the “Lagos de Estaña” area (b).

a) b)

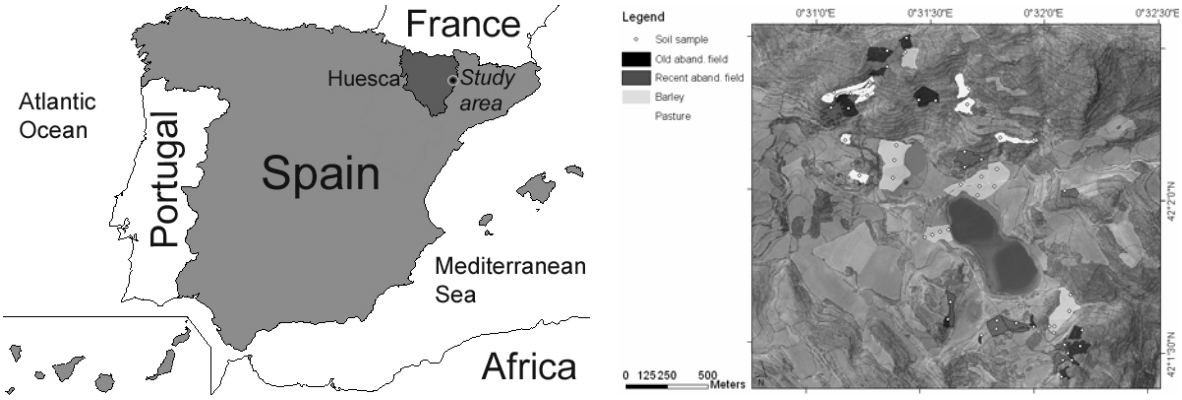

610

611

612

613 Fig. 2. Average monthly rainfall and typical intensities of erosive rainfall (a), and mean monthly number of
614 storm and erosive storm events, and percentage of erosive storm events (b) between 1993 and 2006 in the study
615 area, based on data from the Canelles Weather Station, Spain.

a) b)

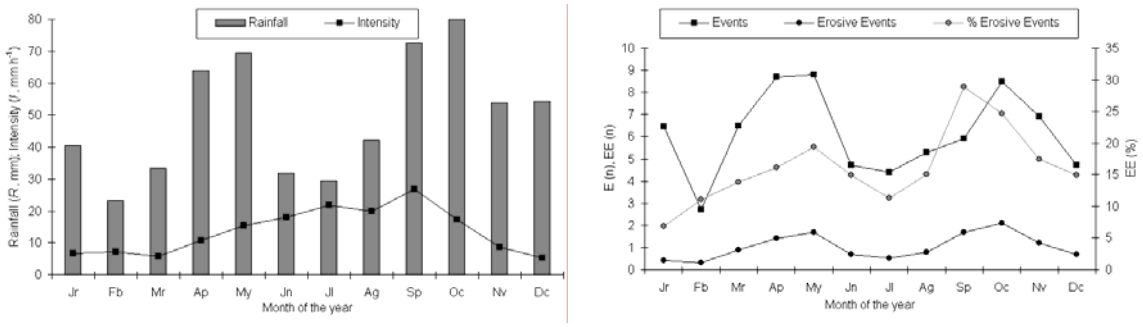

616

Fig. 3. Minimum, maximum, and mean monthly runoff, Q_m *(a)* and effective runoff, $Q_{m\text{-}eff}$, (b) for four types of fields in the south-central Pyrenees, Spain based on the RMMF erosion model.

a) b)

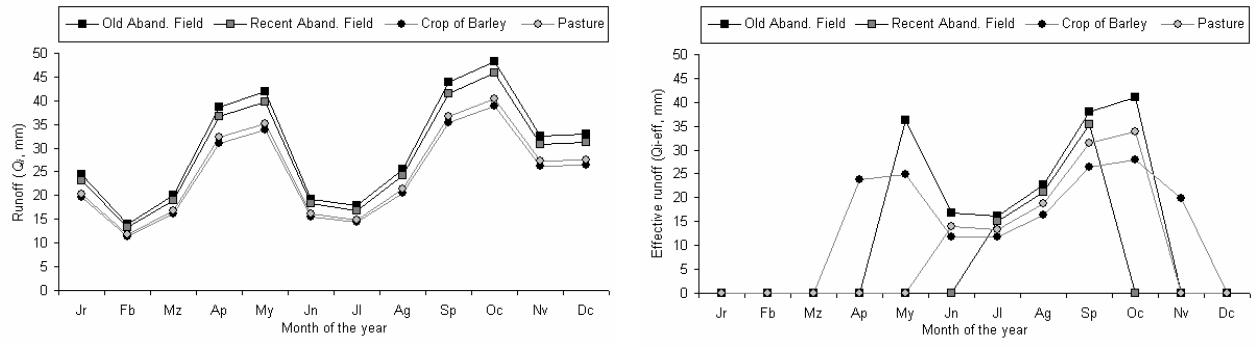

Fig. 4. Textural classification of the soil samples from four types of fields in the south-central Pyrenees, Spain.

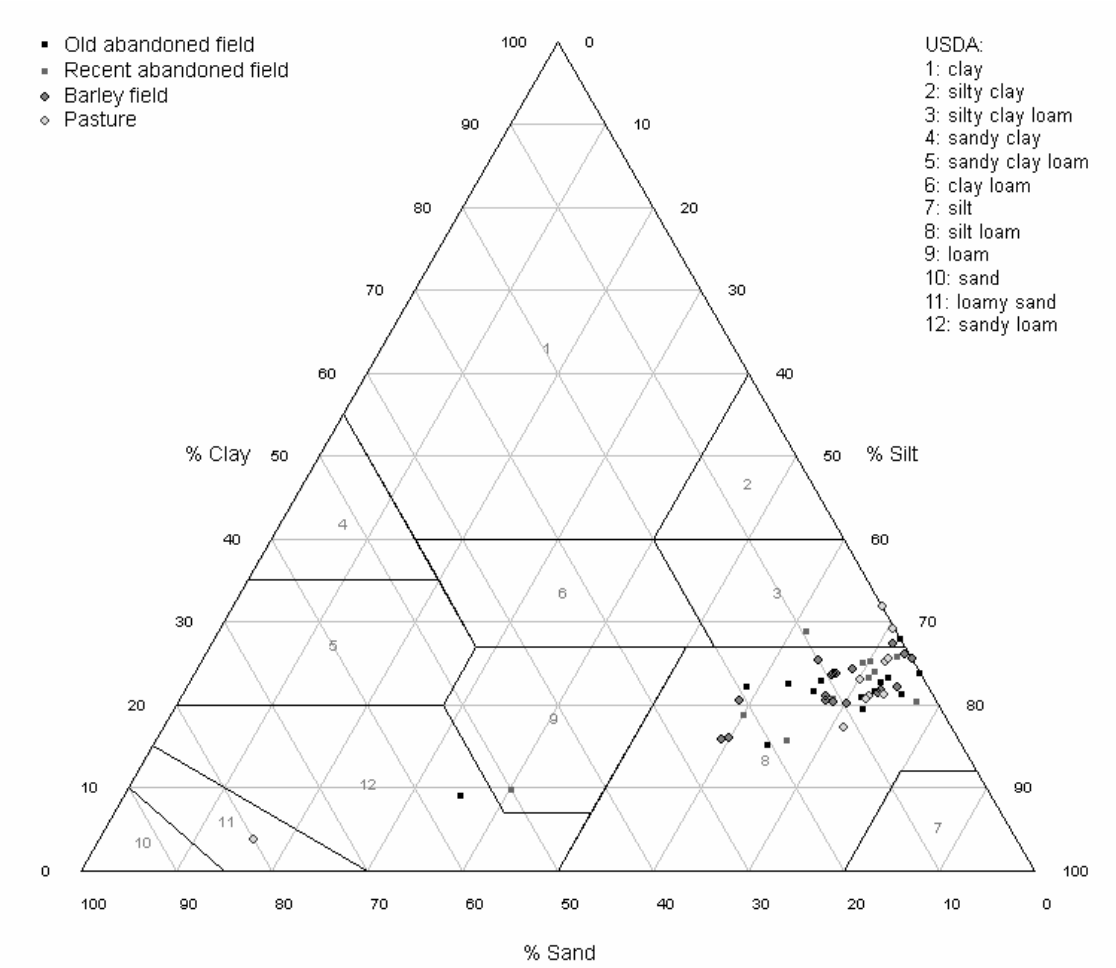

624 Fig. 5. Monthly splash detachment rates (*F*) calculated with the MMF erosion model (a) and with the RMMF
625 erosion model (b), and monthly detachment by runoff (*H*) (c) and total detachment (d) for each of the four field
626 types in the south-central Pyrenees, Spain.

a)

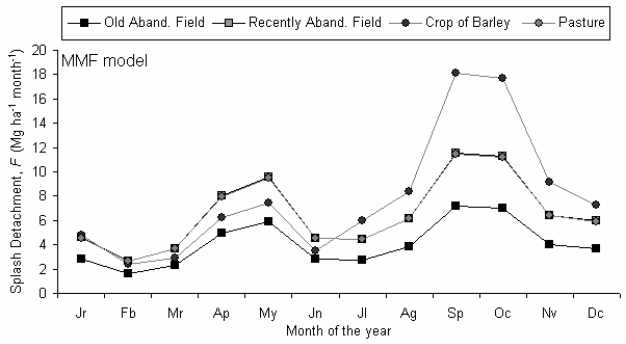

b)

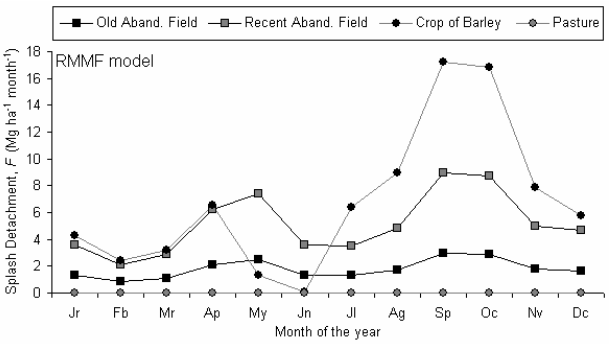

c)

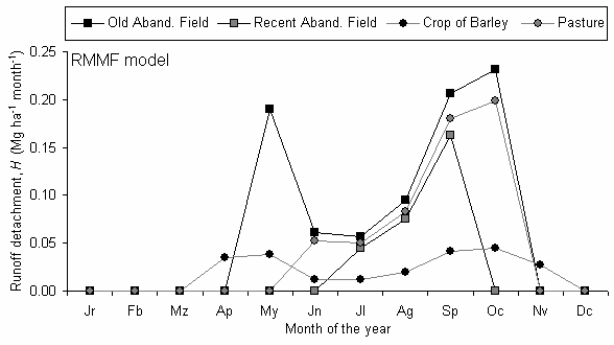

d)

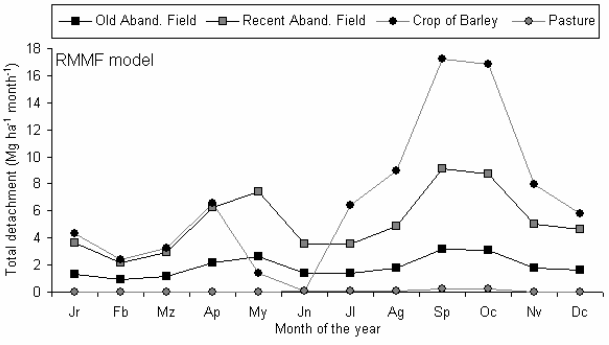

627